Direct Probing by Laser Scanning of the Current Distribution and Inhomogeneity of Josephson Junctions

M. Scheuermann, James R. Lhota, P. K. Kuo, and J. T. Chen
Department of Physics, Wayne State University, Detroit, Michigan 48202
(Received 7 September 1982)

A laser-scanning technique capable of probing the local current density in Josephson junctions has been used to study the current distribution and inhomogeneity of both high- and poor-quality junctions. Results from a high-quality tunnel junction are in good qualitative agreement with theory. The technique is also shown to be useful to study superconduting-normal-superconducting structures and bridge-type weak links.

PACS numbers: 74.50.+r, 74.60.Ge, 74.60.Jg

Up to this time there has been no technique to probe directly the current distribution of Josephson tunnel junctions. Such a probe would provide a method to test theoretical calculations of the spatial distribution of the current density[1-4] as well as a powerful tool for determining and locating inhomogeneities in Josephson junctions. Recently there has developed a vigorous interest in the use of scanning techniques to probe the properties of thin films.[5,6] Chi, Loy, and Cronemeyer[7] have been able to detect inhomogeneities in thin films by studying the zero-voltage current of a laser-induced weak link. The local weak link is created by laser heating of the rest of the superconducting film to normal state. While this experiment gives information about the local properties of the film, it does not yield information about the original current distribution because the geometry of the superconducting portion of the sample has been altered. We have developed a technique which involves scanning a *focused* laser beam to measure local current density and detect inhomogeneities. Unlike the experiment of Chi, Loy, and Cronemeyer where a strong laser field is used to define the geometry of the sample, we have used a weak laser as a *probe* of local current density.

The samples studied were placed in a glass Dewar and immersed in superfluid ^{4}He. Magnetic fields were applied to the samples with a Helmholtz coil which was placed around the Dewar. The focused HeNe laser spot (~20 μm diam and ~1 mW power) is slowly scanned in 1-μm steps across the junction area. At the spot site the local current density is decreased as a result of local heating. Since the maximum zero-voltage current I_0 is the total current, the small perturbation of the local current density at the beam site can be detected by a small change in I_0. If the laser-induced reduction of the local current is proportional to the local current density in the absence of the beam, the small change in I_0 reflects the current density at the beam site. For low beam powers we found good qualitative agreement between the measured current distributions and the theoretically predicted distributions.

A variety of Josephson junctions were studied including Josephson tunnel junctions, superconducting-normal-superconducting structures, and bridge-type weak links. One of the Josephson tunnel junctions studied was an evaporated Pb-PbO-Pb tunnel junction of overlap geometry having a length $L = 0.37$ mm and a width $W = 0.26$ mm. The junction was determined to be of high quality by noting the absence of a zero-voltage current in a large magnetic field and by measuring the I_0 vs applied magnetic field B. At a temperature of 1.3 K the unperturbed I_0 was 31 mA and the Josephson penetration depth λ_j was calculated to be 0.1 mm. Hence for this junction the ratio L/λ_j is 4. The orientations of the laser beam and magnetic field with respect to the sample are shown in Fig. 1. Except for a slight asymmetry, the I_0-vs-B curve was in good qualitative agreement with the calculations of Owen and Scalapino.[1] The slight asymmetry was due to a small self-field. With a scope intensity blanking method, I_0 was recorded as the laser was scanned along the

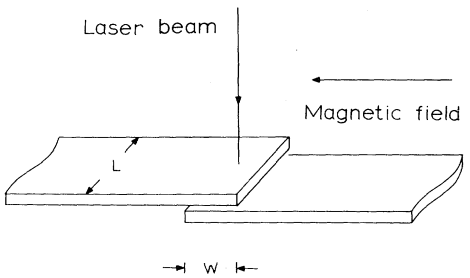

FIG. 1. Orientation of the Josephson tunnel junctions with respect to the laser beam and the applied magnetic field.

length of the junction near the center of the overlap region. The experimental results obtained in this way for several different values of magnetic field are shown in the left column of Fig. 2. Owen and Scalapino have calculated the current distribution inside a Josephson tunnel junction as a function of magnetic field. Using their methods we have calculated the current distribution for the values of reduced magnetic field and the parameter $(L/\lambda_j = 4)$ appropriate for this experiment. The results of the calculation are shown in the right column of Fig. 2 next to the corresponding experimental data. Figure 2(a) shows I_0 versus laser beam position when the magnetic field is adjusted for maximum unperturbed I_0. The measured distribution is in good qualitative agreement with the theoretical result which shows a slight confinement of current near the edges. The slight asymmetry in the current distribution is most likely responsible for the asymmetry in the I_0-vs-B curve as mentioned earlier. This technique can also be used to observe vortex structures in the junction. When a vortex is present in a junction the local current density is positive in some regions while negative in others. Thus the vortex structure is characterized by both a decrease and an *increase* in I_0 with respect to the unperturbed I_0. By an increase in the magnetic field the formation of vortex structures in the junction was observed. The presence of approximately one and a half vortices in the junction can be seen from the distribution shown in Fig. 2(b). As the field was further increased additional vortices appeared. Examples of two and three vortices are shown respectively in Figs. 2(c) and 2(d). These distributions are again in good qualitative agreement with theory. A quantitative comparison with theory depends on the choice of B_{c1}. Since there is no certain way for determining the value of B_{c1} for a long junction of overlap geometry, we have estimated the

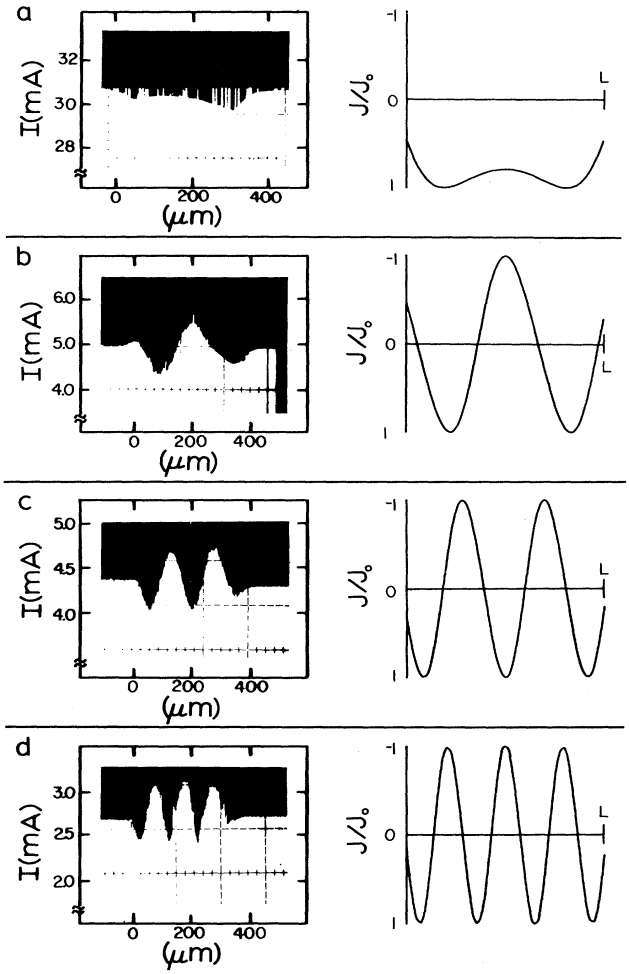

FIG. 2. Figures on the left show maximum zero-voltage current as the beam is scanned across the length of the Pb-PbO_x-Pb junction at various magnetic fields. (a) $I_0 = 31.0$ mA, $B = 0$ G; (b) $I_0 = 5.0$ mA, $B = 1.6$ G; (c) $I_0 = 4.4$ mA, $B = 2.4$ G; (d) $I_0 = 2.7$ mA, $B = 3.4$ G. The maximum zero-voltage current in the absence of the beam is visible at the edges of the photographs where the beam is not on the junction. (The junction extends from 0 to 370 μm.) Spikes in the figures are caused by temporary interruptions of the laser beam by bubbles in the liquid nitrogen. These could be partially eliminated by slowly pumping on the nitrogen bath. Figures on the right show theoretical current distribution.

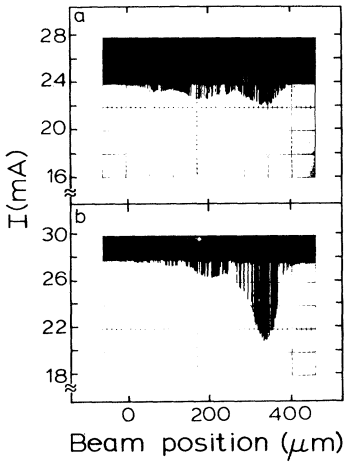

FIG. 3. Maximum zero-voltage current as the beam is scanned across the length of the poor-quality Sn-SnO_x-Sn junction at $T \simeq 1.3$ K. (The junction extends from 0 to 370 μm.) (a) $B = 0$ G; (b) $B = 3.0$ G.

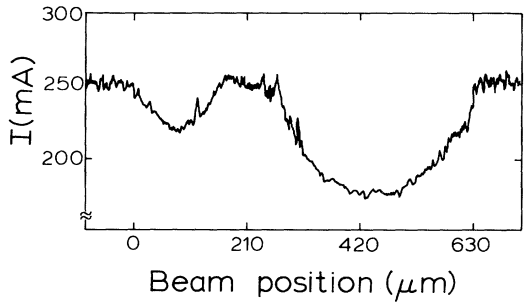

FIG. 4. Maximum zero-voltage current as the beam is scanned across the length of a Sn-Ag-Sn junction at $T = 1.3$ K and $B = 0$. (The superconducting-normal-superconducting structure extends from 0 to 630 μm.)

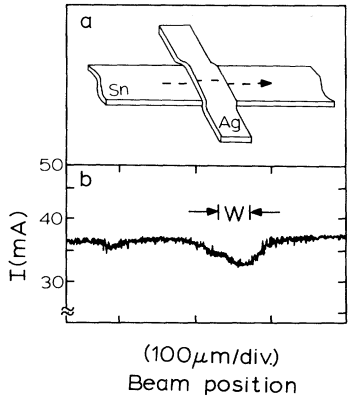

FIG. 5. (a) Geometry of a superconducting strip with normal overlay. The arrow indicates the line along which the laser beam was scanned. (b) The maximum zero-voltage current of a bridge-type weak link as the beam is scanned across a portion of the bridge. The region labeled W is the position of a normal-metal overlay.

value of B_{c1} to be 0.7 G which gives a good overall fit as shown.

This technique was also used to probe nonuniformities of a poor-quality Sn-SnO-Sn tunnel junction of the same geometry and dimensions. The poor quality was inferred by a large leakage current. Figure 3(a) shows the current distribution in the absence of an applied magnetic field. The observed distribution differs grossly from that expected for a high-quality junction. In an applied magnetic field, changes in the distribution were observed as seen in Fig. 3(b). However the formation of vortices was not observed until the fields applied were much larger than theoretically expected. We expect that future improvements in resolution will make this a useful tool in detecting inhomogeneities in the oxide layer.

Nonuniformities in the current distribution of a Sn-Ag-Sn structure were also observed. Using a sample-and-hold method to record I_0, we measured the current distribution across the width of the sample which is shown in Fig. 4. We have also used this technique to study bridge-type weak links. For example the presence of a small normal overlay has been detected, as shown in Fig. 5. The region labeled W shows the position of a normal overlay on the bridge which was easily detected as the beam passed. Note that because of the proximity effect the weakened portion of the bridge is nearly twice the width of the overlay. The other reduction in the zero-voltage current to the left of the overlay is due to some unknown inhomogeneity in the bridge.

Laser-induced changes in the quasiparticle current-voltage characteristics have also been used to probe inhomogeneities in Josephson tunnel junctions. By biasing with a constant current source to near the gap voltage, we measure a small voltage difference ΔV between the presence and absence of the beam. Scanning with a chopped laser beam, we have detected inhomogeneities by measuring variations in ΔV. Alternatively one could bias at a constant voltage and measure variations in the change of the current.

In conclusion we have demonstrated this technique to be a powerful tool for probing the local current density of Josephson devices. Other applications include probing nonequilibrium quasiparticle distributions, studying the effects of cavity and vortex modes in Josephson tunnel junctions, and studying phase slip centers in bridge-type weak links. Improvements in the mechanics of this technique should make it a useful tool for detecting and locating inhomogeneities in tunnel junctions and thin films at low temperatures.

We would like to thank Jhy-Jiun Chang for useful discussions. This work was supported by the National Science Foundation through Grant No. DMR-80-24052.

[1]C. S. Owen and D. J. Scalapino, Phys. Rev. 164, 538 (1967).

[2]J. Matisoo, J. Appl. Phys. 40, 1813 (1969).

[3]A. Barone, W. J. Johnson, and R. Vaglio, J. Appl. Phys. 46, 3628 (1975).

[4]A. Barone, F. Esposito, K. K. Likharev, V. K. Semenov, B. N. Todorov, and R. Vaglio, "Effect of Boundary Conditions upon the Phase Distribution in Two-Dimensional Josephson Junctions," to be pub-

lished.
[5]R. Eichele, H. Seifert, and R. P. Huebner, Appl. Phys. Lett. 38, 383 (1981).
[6]P. L. Stöhr, Appl. Phys. Lett. 39, 828 (1981).
[7]C. C. Chi, M. M. T. Loy, and D. C. Cronemeyer, Appl. Phys. Lett. 40, 437 (1982).

Anomalous Diffusion on Percolating Clusters

Yuval Gefen and Amnon Aharony
Department of Physics and Astronomy, Tel Aviv University, Ramat Aviv, Israel

and

Shlomo Alexander
The Racah Institute of Physics, The Hebrew University, Jerusalem, Israel
(Received 7 September 1982)

The mean square distance reached after t random-walk steps on a percolating cluster is shown to behave as $t^{2/(2+\theta)}$ (instead of t) for short times (for which the cluster is seen to be self-similar). The exponent θ is related to that describing the dc conductivity near percolation. Averaging over all clusters yields the ac conductivity and dielectric constant near percolation in the high-frequency limit, when the polarization of the medium is unimportant.

PACS numbers: 71.30.+h, 05.50.+q

Much of the current interest in the properties of dilute systems concentrates on the vicinity of the percolation threshold, p_c.[1,2] As the concentration p of, e.g., conducting links, in a metal-insulator alloy, approaches p_c, the percolation correlation (i.e., the pair connectedness) length diverges as $\xi \sim |p-p_c|^{-\nu}$. For $p>p_c$, the probability to belong to the infinite cluster is $P_\infty(p) \propto (p-p_c)^\beta \propto \xi^{-\beta/\nu}$ and the dc conductivity approaches zero as $\sigma_{dc} \propto (p-p_c)^\mu \propto \xi^{-\mu/\nu}$. Both P_∞ and σ_{dc} vanish for $p<p_c$. In a superconductor–normal-metal alloy, one has $\sigma_{dc} \propto (p_c-p)^{-s}$ for $p<p_c$. The exponent s has recently also been predicted to describe the divergence of the dielectric constant of a metal-insulator alloy as p_c is approached from below.[3,4]

All these results represent *macroscopic* averages, taken over samples which are *large compared to* ξ. On such large length scales, the samples look *homogeneous*. However, both Monte Carlo simulations[2] and experiments[5] show that the geometry of the percolating cluster is not homogeneous for length scales L which are in the range $a \ll L \ll \xi$ (a is the microscopic lattice distance). In this range the clusters are *self-similar*, and the number of links which belong to a given cluster (whose size is larger than L) within a volume L^d (in d dimensions) varies as L^{d_f}, with the fractal dimensionality $d_f = d - \beta/\nu$.[2,6,7] Note that this property is expected of both the finite and the infinite clusters. On "anomalous" length scales L, with $a \ll L \ll \xi$, one expects all physical measurements to reflect this self-similarity and to yield results which behave as powers of L, *independent* of ξ.[7] Bulk properties are then found by a juxtaposition of pieces of size ξ. The aim of the present Letter is to use scaling considerations for deducing these "anomalous" properties and the crossover at $L \approx \xi$.[8]

Our main results concern the problem of diffusion on random networks ("the unbiased ant in the labyrinth").[9-12] Consider a single percolation cluster, containing s sites within a linear range of order $r_s \propto s^{1/d_f}$. If the random walker (the "ant") is put on this cluster, and if the distance it travels after t time steps, $r(t)$, satisfies $a \ll r(t) \ll (r_s, \xi)$, then self-similarity implies that

$$\langle r^2(t) \rangle_s = A^2 t^{2/(2+\theta)}, \tag{1}$$

for *both* $p>p_c$ and $p<p_c$. One may define an *effective dimensionality of the random walk*,[13] d_{rw}, via $t \propto r^{d_{rw}}$. Our result implies that $d_{rw} = 2+\theta$, instead of the usual Fickian value $d_{rw}=2$ (i.e., $\langle r^2 \rangle \propto t$). (In the notation of Ref. 6, Chaps. 27–30, $2+\theta = 1/H$.) The latter is recovered only for $p>p_c$ and $r(t) \gg \xi$. The exponent θ is given by $\theta = (\mu-\beta)/\nu$. Using known estimates for μ, β,